Temperature Effects on the Dissociative Electron Attachment to Dichlorobenzene Isomers[†]

M. Mahmoodi-Darian, A. Mauracher, A. Aleem, S. Denifl, B. Rittenschober, A. Bacher, M. Probst, T. D. Märk,* and P. Scheier

Institut für Ionenphysik und Angewandte Physik, Leopold-Franzens Universität Innsbruck, Technikerstrasse 25, A-6020 Innsbruck, Austria

Received: May 29, 2009; Revised Manuscript Received: October 14, 2009

Dissociative electron attachment to all three isomers of dichlorobenzene has been investigated in the electron energy range from 0 to 2 eV and in the gas temperature range from 391 to 696 K using a crossed electron-molecular beam apparatus with a new temperature-regulated effusive molecular beam source. In the case of the dissociative electron attachment channel Cl^-/1,2-dichlorobenzene and Cl^-/1,4-dichlorobenzene, strong enhancement of the negative ion production with the gas temperature at low electron energies has been observed. The low-energy peak increases dramatically when the gas temperature is raised from 391 to 696 K. Activation energies for dissociative electron attachment of (482 ± 20) meV for 1,2-dichlorobenzene and (59 ± 20) meV for 1,4-dichlorobenzene have been determined. For the resonance at (0.49 ± 0.03) eV in 1,2-dichlorobenzene and (0.32 ± 0.03) eV in 1,4-dichlorobenzene, no dependence of the cross sections on the gas temperature has been observed. In the case of the dissociative electron attachment to Cl^-/1,3-dichlorobenzene, the cross section does not depend on the temperature in the electron energy range from 0 to 2 eV. Quantum chemical calculations of the reaction energies and of the potential energy curves involved in the dissociation of Cl^- have been performed, together with an analysis of the thermo dynamical accessibility of the relevant vibrational modes. Possible reasons for the different temperature dependences of the isomers are discussed.

Introduction

Dissociative electron attachment (DEA) to molecules is often a very effective reaction and responsible, for example, for negative ion formation in plasmas.[1] DEA to halogenated hydrocarbons in many cases is exothermic, and hence, already low-energy electrons are able to ionize and dissociate the corresponding molecules. The rate coefficients in many exothermic DEA reactions depend sensitively on both the electron and gas temperature.[2] The reactive species produced, a halogen anion, X^-, and a hydrocarbon radical, M, play an important role in dry etching plasmas used in VLSI (very large scale integration) manufacturing and in excimer and chemical laser plasmas. Moreover, such species are possibly also involved in the processes leading to ozone depletion in the atmosphere. Furthermore, there exists a similarity between DEA to halohydrocarbons and the process of reductive dehalogenation promoted by bacteria in anaerobic sediments, sewage sludge, and aquifer materials.[3] Therefore, understanding the energetics and dynamics of DEA to these molecules XM is important also for possible improvements in technological applications as well as for understanding and better control of environmental processes. Knowledge of the electron energy dependence of the DEA cross section as well as its dependence on the gas temperature is essential to describe these mentioned processes.

In this contribution, we study systematically the influence of the temperature on electron attachment processes for some halohydrocarbon molecules. The experiment involves a crossed electron/molecular beam arrangement with a mass spectrometric detection for the anions formed.

If free electrons interact with neutral molecules, XM, a temporary negative ion (TNI) can be formed by resonant electron capture.[1,4,5]

$$e^- + XM \rightarrow XM^{-(*)} \quad (1)$$

Such an attachment process usually occurs within a restricted energy range, since it represents a transition from a continuum state to a discrete electronic state. A negative ion state thereby formed is embedded in its autodetachment continuum and is, hence, principally unstable toward autodetachment (AD). We note, however, that the picture for electron attachment via Franck−Condon transitions between localized potential energy surfaces may become inadequate at very low electron energies (breakdown of the Born−Oppenheimer approximation) and also in large systems having a high density of states. In the latter case, the electronic energy (comprising the energy of the incoming electron plus the electron affinity of the target molecule) can directly and effectively be dispersed into the many vibrational degrees of freedom. In this contribution, we are restricted to gas-phase molecules under collision-free conditions. Under such conditions, a TNI usually relaxes via autodetachment (the reverse of eq 1, AD) or via unimolecular decomposition into thermodynamically stable fragments $M + X^-$ (DEA). It has been known for as long as three decades that the temperature may have a strong effect on DEA. This is mainly due to the fact that the formation of the TNI is coupled to vibrational excitation. Thus, the occupation of the vibrational states of the neutral molecule can have strong effects on their fragmentation. How this influence manifests itself in the ion yield curves of the individual fragments is complex and depends largely on the relative disposition of the involved neutral and anionic potential energy surfaces.[1,5] Heating of the molecule and, thus, increasing

[†] Part of the "Vincenzo Aquilanti Festschrift".

* Corresponding author. Fax: +43 512 507 2932. E-mail: tilmann.maerk@uibk.ac.at.

10.1021/jp9050726
Published on Web 10/30/2009

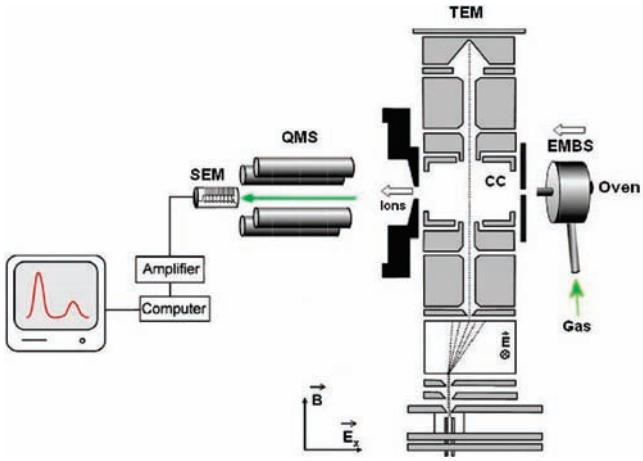

Figure 1. Schematic view of the electron−molecular beam apparatus.

the population of vibrationally excited states extends the Franck−Condon region, thus allowing transitions to the repulsive ionic potential energy curve at lower electron energies and, hence, resulting in higher dissociation probability. In addition, the temperature dependence reflects the thermodynamics of the particular dissociative attachment reaction and also gives some insight into the underlying mechanisms and dynamics.

DEA reactions can be either (i) exothermic or (ii) endothermic. The present cases are endothermic. In the case of an endothermic DEA reaction, an activation energy (AE) exists. The presence of the AE can hinder the dissociation of the TNI at electron energies of ≈0 eV, and the DEA cross section then depends strongly on T at these energies. In this case, the dependence of the ion signal on the temperature T at very low electron energies is described by the Arrhenius equation,

$$I(T) = I_0 \cdot \exp\left(-\frac{E_A}{k_B T}\right) \quad (2)$$

where $I(T)$ is the ion current close to 0 eV and k_B is the Boltzmann constant. For reactions without an AE, the cross section for DEA reactions at low electron energies does not depend on T.

Experiment

The present study has been carried out using a high-resolution electron−molecular beam apparatus. A schematic of the apparatus is shown in Figure 1. The electron beam formed by a trochoidal electron monochromator (TEM) and accelerated to selected electron energy is crossed by a molecular beam formed by an effusive molecular beam source (EMBS). The negative ions produced in the collision chamber (CC) are extracted by a weak electric field from the interaction region and focused into the entrance of the quadrupole mass spectrometer (QMS). The mass-selected negative ions are detected as a function of the electron energy in a single ion counting mode using a secondary electron multiplier (SEM), ion counting electronics, and a PC acquisition system.[6] The entire system is situated in a high-vacuum chamber that is pumped by a 300 L/s turbo-molecular pump. Three halogen lamps inside the vacuum chamber are used as internal heaters to keep the surfaces clean (base pressure of the apparatus, $P < 10^{-6}$ Pa). During the measurements, when the gas flow through EMBS into the vacuum chamber is established, the pressure in the main vacuum chamber is usually below 10^{-4} Pa.

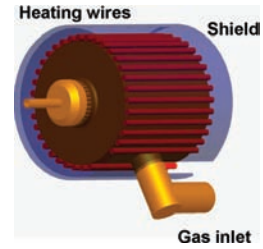

Figure 2. Schematic view of the effusive molecular beam source.

The TEM invented by Stamatovic and Schulz[7] has been used as a source for production of almost monoenergetic electrons. Regarding the monochromator, we use a hairpin filament that is specified to produce an electron distribution of 700 meV. Electrons are emitted thermally from the filament tip, extracted by an electric field of several volts per millimeter, and guided by an axial magnetic field of up to 5 mT. The magnetic field is produced by two solenoids that are 765 mm in diameter and 270 mm apart from each other and are mounted at the outside of the vacuum vessel. Typical electron emission currents are on the order of several microamps. After passing two electrostatic lenses with orifices of 1 mm diameter, the beam enters the dispersive element, where a weak electrostatic deflection field of about 100 V m^{-1} perpendicular to the magnetic field is applied. According to the trochoidal principle, the electrons are deflected depending on the time spent in the dispersive element; that is, their kinetic energy in the forward direction. Subsequently, at the exit of the dispersive element, only part of the electron distribution is allowed to pass through the orifice in the exit electrode. These electrons are then accelerated to the desired energy and enter the collision chamber, where the monochromatic electron beam is crossed by a molecular beam. The anions produced by the electron attachment processes are weakly extracted into a quadrupole mass filter, where they can be analyzed and detected. After crossing the collision region, the remaining electrons are collected, and the electron current is monitored online during the experiment using a picoelectrometer.

The effusive molecular beam source that has been developed for the present measurements (Figure 2) consists of a heated stainless steel gas container (volume ≈ 11 cm^3) in cylindrical shape. The pressure inside the EMBS is measured with a pressure sensor (pressure range $0-10^{-2}$ Pa). A well-defined molecular beam with a narrow angular distribution function is formed by effusion of the molecules through a capillary 0.9 mm in diameter and 2 mm in length at the tip of the cylinder. The EMBS is resistively heated using 11 heaters made from ceramic tubes and tungsten wire. The temperature of the EMBS is measured by PT100. A small, stainless steel container containing the samples is connected to the EMBS through a needle valve and a metering bellows-sealed valve, reducing the gas pressure. At the pressures used here, the mean free path of the molecules in the EMBS is much longer than the typical dimension of the EMBS, and thus, the collisions of the molecules with the walls are dominant. We assume that the molecules are in thermal equilibrium with the walls of the EMBS, and thus, the temperature of the molecules is equal to the temperature of the walls measured by the temperature sensor. If the gas flow through the EMBS is constant, the density of the gas in the molecular beam, n_0, varies with the temperature of EMBS (hence, T) according to following expression:

$$n_0 \propto T^{-0.5} \quad (3)$$

If a cross section for DEA does not depend on T, the ion current will follow this dependence. To test the new oven and temperature dependency, we decided to measure a well-known temperature-dependent fragment Cl^- formed by $CHCl_3$. The AE of $Cl^-/CHCl_3$ calculated from the present data is about 146 meV, which is in good agreement with another value determined recently with a hemispherical monochromator in our laboratories (150 ± 20 meV).[8]

Calibration of the electron energy scale and estimation of the electron energy distribution function of the electrons for the whole measurements mentioned in the paper have been performed using the EA reaction:

$$e^- + SF_6 \rightarrow (SF_6)^{*-} \quad (4)$$

This molecule possesses at ≈0 eV a very high attachment cross section due to s-wave attachment. The transient negative ion $(SF_6)^{*-}$ can be detected in a mass spectroscopic experiment due to its lifetime extending to ms. For these reasons, SF_6^- can be used for the calibration of electron energy scale as well as for the estimation of the spread of the electron energy distribution function in crossed beam experiments. The measured resonance with a finite width is due to the convolution of the attachment cross section and the electron energy distribution function. The maximum of the peak is set as zero electron energy, and the width of the peak at the half-maximum (fwhm) is a measure of the electron energy distribution.

In the present work, the gas temperature dependencies of the DEA have been studied for 1,2-dichlorobenzene, 1,3-dichlorobenzene, and 1,4-dichlorobenzene molecules that had been obtained from Sigma Aldrich with a stated purity of ≥99% without further purification.

Results

A. 1,2-$C_6H_4Cl_2$ (1,2-ΦCl_2). No parent molecular anion can be detected in our crossed-beam experiment at low electron energies (below 2 eV); that is, the lifetime of the TNI $(1,2\text{-}\Phi Cl_2)^{*-}$ is too short to allow detection. The only negatively charged product of DEA reactions in the low electron energy range, observed in the present crossed beams experiment, is Cl^-. The cross section for DEA to 1,2-ΦCl_2 at low temperature has one peak around (0.49 ± 0.03) eV due to the DEA process to the repulsive part of the negative ion state. As temperature increases, the threshold peak grows at very low energies due to DEA induced by a capture of slow s-wave electrons.

Ion efficiency curves have been measured in the gas temperature range between 412 and 696 K and with an electron energy resolution of about 66 meV (fwhm). The anion yield shows a low energy resonance that exclusively shows one decay channel that results from the cleavage of the C−Cl bond

$$e^- + 1,2\text{-}C_6H_4Cl_2 \rightarrow [1,2\text{-}C_6H_4Cl_2]^{*-} \rightarrow 1,2\text{-}C_6H_4Cl^{\bullet} + Cl^- \quad (5)$$

Figure 3 displays the electron energy dependence of the relative cross sections for the fragment ion Cl^- observed from 1,2-$C_6H_4Cl_2$ recorded at different temperatures. By increasing the temperature, a narrow feature close to 0 eV appears. Strong temperature dependence of the zero energy peak is evident from

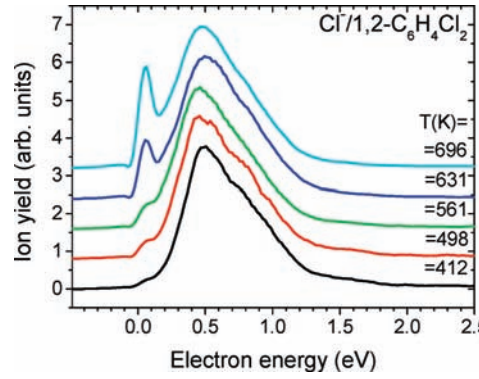

Figure 3. Dependence of Cl^- yield due to DEA to 1,2-ΦCl_2 (measured with the TEM setup, resolution ~66 meV) on the gas temperature over the range $T = 412-696$ K. The respective anion yields were normalized to the same value at the higher energy peak and are shifted by adding a constant value to each subsequent spectrum for clarity.

Figure 3. The energetic threshold for the formation of the observed ionic fragment Cl^- is 0.69 eV calculated by means of the G3(MP2) method.[9] Within the uncertainty of the method (0.15 eV), the same energy was obtained for the three isomers as reactants in reaction 5. It should be noted that in endothermic DEA reactions, peaks can, in fact, appear near 0 eV due to processes involving vibrationally excited states.

In the case of an Arrhenius-like behavior, the activation barrier can be deduced from the dependence of the low-energy feature with the gas temperature. A plot of the logarithm of the Cl^- threshold intensity vs $1/T$, in fact, shows a linear dependence, thus leading to the activation energy. An Arrhenius plot for the zero energy peak of the 1,2-ΦCl_2 molecule is presented in Figure 4a. From the slope of the Arrhenius plot, an activation energy for DEA to 1,2-ΦCl_2 of (482.4 ± 20) meV has been deduced. The uncertainty has been calculated during the fitting process of the regression line to the data points and is for all fits below the given value of ±20 meV. The count rates have been multiplied by the factor $\sqrt{(T/T_0)}$ ($T_0 = 498$ K) to correct for the varying gas density with temperature in the collision zone.

Although the low-energy Cl^- signal shows a strong temperature effect, the other channels, including Cl^- from the second resonance, are virtually unaffected by an increase in the gas temperature (Figure 4b). The present experiments demonstrate that the cross section for DEA associated with direct electronic dissociation can vary strongly with the temperature of the target molecule. For systems having an activation barrier, an increase in the temperature results in a shift and a concomitant increase in the anion yield and the appearance of a low-energy feature. This threshold peak arises from transitions close to the crossing point having survival probabilities near unity. Its temperature dependence simply mirrors the population of vibrational states according to the Boltzmann distribution at the level of the crossing point and, hence, obeys an Arrhenius-like behavior.

B. 1,3-$C_6H_4Cl_2$ (1,3-ΦCl_2). DEA to 1,3-dichlorobenzene has been measured as a function of the electron energy and the gas temperature with an electron energy resolution of 130 meV (fwhm). The Cl^- ion yield as a function of electron energy (Figure 5a) exhibits one peak, at (0.39 ± 0.07) eV. The calculated energetic threshold by means of G3(MP2)[9] calculations is 0.68 eV. The gas temperature dependence of the peak in the temperature range 395−516 K is shown in Figure 5b. In the temperature range 395−516 K, the intensity of the peak varies with the gas temperature as $T^{-0.5}$. Thus, in this temperature range, the cross section for DEA to 1,3-ΦCl_2 does not depend on T.

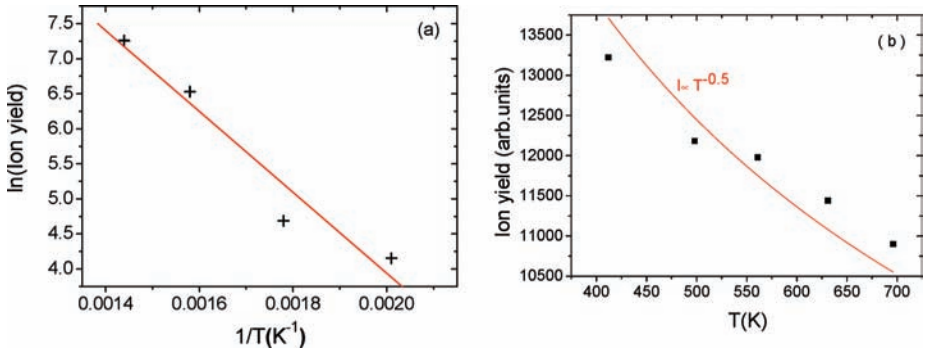

Figure 4. (a) Arrhenius plot of the threshold intensity. The slope of the straight line corresponds to an activation energy for Cl^- formation of 482.4 meV. The intensities are corrected for the $T^{-0.5}$ dependence of the gas density in the reaction volume. (b) Cl^- ion yield at the 0.49 eV resonance in 1,2-ΦCl_2 as the function of T (full squares). The solid line represents a fit to the experimental data based on a $T^{-0.5}$ dependence.

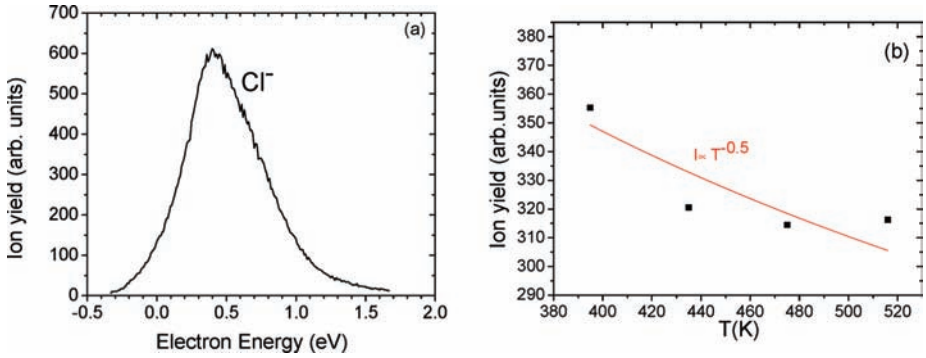

Figure 5. (a) Ion yield curve for the DEA reaction Cl^-/1,3-ΦCl_2 at 395 K. (b) Cl^-/1,3-ΦCl_2 intensity of the peak as a function of T (■). The solid line represents a fit to the experimental data basing on a $T^{-0.5}$ dependence.

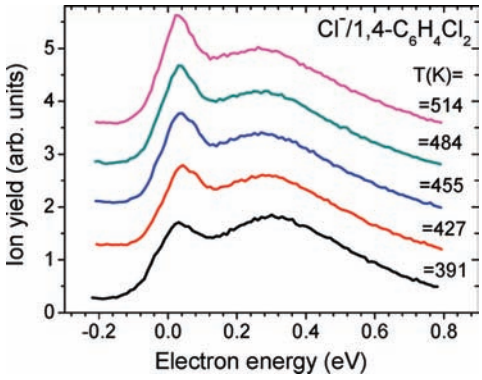

Figure 6. Dependence of Cl^- yield due to DEA to 1,4-ΦCl_2 (measured with the TEM setup, resolution ~83 meV) on the gas temperature over the range $T = 391-514$ K. The respective anion yields were normalized to the same value at the higher energy peak and are shifted by adding a constant value to each subsequent spectrum for clarity.

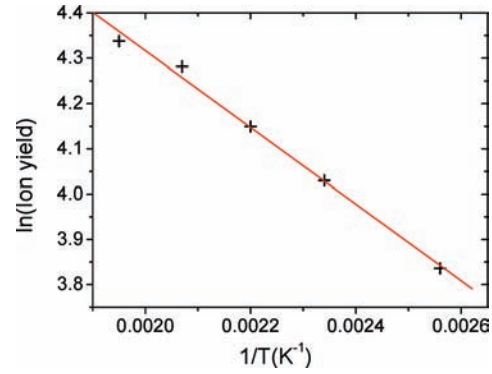

Figure 7. Arrhenius plot of the threshold intensity. The slope of the straight line corresponds to an activation energy for Cl^- formation of 59.42 meV. The intensities are corrected for the $T^{-0.5}$ dependence of the gas density in the reaction volume.

C. 1,4-$C_6H_4Cl_2$ (1,4-ΦCl_2). Figure 6 shows the ion yields for the negative ion Cl^- recorded at gas temperatures within the range of 391−514 K. Cl^- is the only negative ion observable from 1,4-ΦCl_2 in the present experiment in the electron energy range from 0 to 2 eV. No molecular ion was observed within the sensitivity of the apparatus. The ion yield peaks at energies close to zero and (0.32 ± 0.03) eV. The electron energy resolution was about 80 meV. The energetic threshold for the formation of the observed ionic fragment Cl^- derived from G3(MP2) calculations[9] is 0.70 eV. It should be noted that near threshold (0 eV), the shape of the ion yield is strongly affected by the electron energy distribution function: in comparison to 1,2-ΦCl_2, one can see that the threshold peak for 1,2-ΦCl_2 is narrower than for 1,4-ΦCl_2. This can be explained by the slightly better electron energy resolution (66 meV) for the 1,2-ΦCl_2 isomer. The positions of the DEA peaks have been obtained by nonlinear least-squares fitting of the Gaussian functions to the ion yields. An Arrhenius-type plot of the maximum intensity of the peak at zero energy yields an activation energy of (59 ± 20) meV (Figure 7).

For the peak at 0.32 eV, we observe a decrease in the count rate with increasing temperature following the $T^{-0.5}$ behavior, indicating that the DEA cross section via the second resonance is insensitive to temperature (Figure 8).

Theoretical Considerations

The theoretical relationship between a one-dimensional reaction coordinate and Arrhenius plots has been outlined recently by Fabrikant and Hotop[10] and indicates that caution should be exercised when applying the Arrhenius equation to DEA reactions.

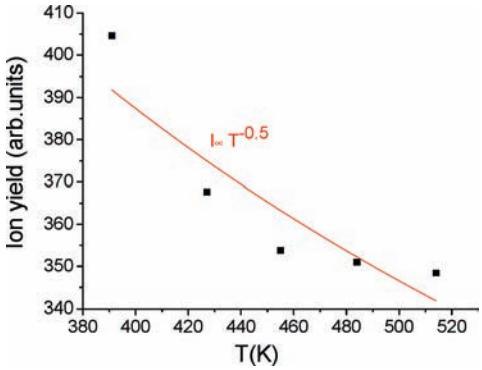

Figure 8. Cl^- ion yield at the 0.32 eV resonance in 1,4-ΦCl_2 as a function of T (■). The solid line represents a fit to the experimental data based on $T^{-0.5}$ dependence.

To our knowledge, the only work in which electron attachment to dichlorobenzene isomers has been discussed is ref 11, in which electron transmission spectroscopy (ETS) and theoretical considerations were used to determine the energies of their metastable anions. Miller[12] studied the rate constants for the formation of trifluorobenzonitrile anions and found large differences for the three isomers. As in our systems, the order of the rates does not follow the simple resonance stabilization arguments from organic chemistry from which the 1-3 isomer should be least reactive.

Monochlorobenzene has been a prototype molecule in DEA studies, starting with the paper of Clarce and Coulson,[13] which is perhaps the first one to describe the qualitative features of the relevant potential curves. Modelli and Venuti[14] compared calculated and measured (ETS) energies of the anion states for chlorobenzene, benzylchloride, and 2-Cl-ethylbenzene. Their data support the generally accepted idea that the captured electron occupies at first a π^* orbital before moving to the C−Cl σ^* molecular orbital (MO), which leads to subsequent dissociation of Cl^-. The coupling of these π^* and Cl σ^* MOs was investigated in more detail in ref 15. This was also done from a theoretical viewpoint in ref 16 with application to DEA of NC-Φ-Cl in solution. There, the conical intersection between the π^* and σ^* surfaces of the anion as functions of the Cl-Φ out-of-plane (oop) angle $\theta_{Cl\text{-}\Phi}$ and the C−Cl distance were calculated. There is agreement that chlorobenzene is a planar molecule, and the electron transfer to the C−Cl σ^* MO is made possible by vibronic coupling. Once the electron is transferred, the dissociation proceeds barrierless.

We are not aware of an experimental or theoretical study of the temperature dependence of the dissociation mechanism in dichlorobenzenes or in similar molecules. A temperature dependence as observed here for the 1,2 and 1,4 isomers could result from a larger π^* to σ^* transition, probability due to larger geometry changes in the oop vibrations together with the larger probability of the anion to access the repulsive dissociative part of the adiabatic C−Cl potential energy curve. The latter would indicate a different situation, as compared to chlorobenzene discussed above. A calculation of the DEA rate as a function of temperature or even to quantify the reasons for the differences between the three isomers is virtually impossible.

However, we can look at (a) the vibrational energies and the temperatures required for exciting them, (b) the shape of the relevant vibrations, and (c) the adiabatic potential energy curves.

Thermal and Vibrational Energies. We calculated the vibrational frequencies of the neutral *o*-, *m*-, and *p*-ΦCl_2 isomers at the B3LYP/cc-pVTZ level of theory and identified the Cl out-of-plane bending modes and the normal modes dominated by a C−Cl stretching vibration. Their energies were compared with the thermal energy in our experiments. The probability, p, of finding a molecule with energy E in a system of temperature T is given by

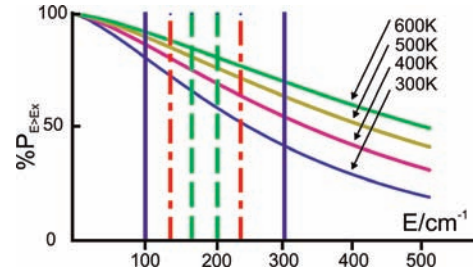

Figure 9. Percentages of molecules with thermal energies larger than the corresponding x-axis value at temperatures of 300, 400, 500, and 600 K. The vertical bars show the energies required to excite the oop vibrations of 1,2 (dashed−dotted lines), 1,3 (dashed lines), and 1,4-Φ-Cl_2 (solid lines).

$$p(E,T) = 2\sqrt{\frac{E}{\pi(Tk_B)^3}}e^{-E/Tk_B} \quad (6)$$

where k_B is Boltzmann's constant. Accordingly, the number of molecules with a higher energy than E at a temperature T is given by the probability, P

$$P(E,T) = 1 - \int_0^E p(E',T)\,dE' \quad (7)$$

In Figure 9, $P(E, T)$ is given for the temperatures 300 (blue curve) to 600 (green) K. Energies (x-axis) are plotted in cm^{-1} for easy comparison with the vibrational levels, and the probabilities (y-axis) are given as $\%P(E, T)$. One electronvolt corresponds to 8065 cm^{-1}. Additionally, for each of the three isomers, the vibrational energy of the symmetric and the antisymmetric Φ-Cl oop mode is indicated by a vertical bar. Since the $\theta_{Cl\text{-}\Phi}$ force constants in the three isomers are similar, the symmetric (at lower energy) antisymmetric (higher energy) modes split from a common center at ∼190 cm^{-1}.

Figure 9 shows that even at 300 K, ∼80% of the molecules have enough energy to excite the symmetric oop mode of *p*-ΦCl_2 which is the mode with the lowest frequency, and in 40%, the symmetric oop mode of *p*-ΦCl_2 can be excited. The other ratios lie between. It also shows that all Cl-Φ oop modes are in the energy range where $P(E, T)$ have the largest energy dependence; that is, in the middle region of their sigmoidal shape. One can also see that the higher states of each mode have still finite probablility to be excited.

Vibrational Modes. Despite their formal similarity, the oop modes lead to very different distortions of the benzene rings due to the high mass of Cl and the different symmetries of the isomers. The frequencies of the oop modes and C−Cl stretching for the neutral isomers are given in Figure 10, together with pictures of the atomic displacement vectors. The 1,4 and 1,2 isomers have the lowest oop frequencies (102 and 137 cm^{-1}, respectively).

Potential Energy As a Function of the C−Cl Distance. At the optimized geometry of the neutral molecule, the anion has a negative electron affinity. However, we did not perform calculations in the metastable domain because it has, for

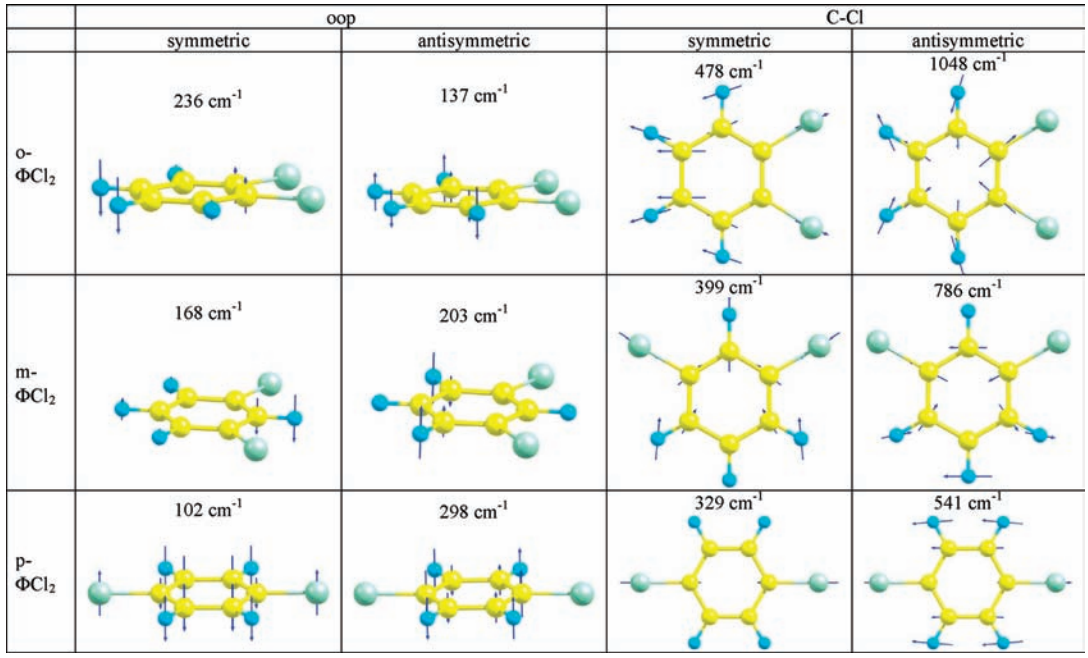

Figure 10. Normal modes and frequencies of the oop and C−Cl vibrations of the three isomers (B3LYP/cc-pVTZ calculations). The oop vibration of ΦCl is at 189 cm^{-1}, and C−Cl stretching vibration is at 415 cm^{-1}.

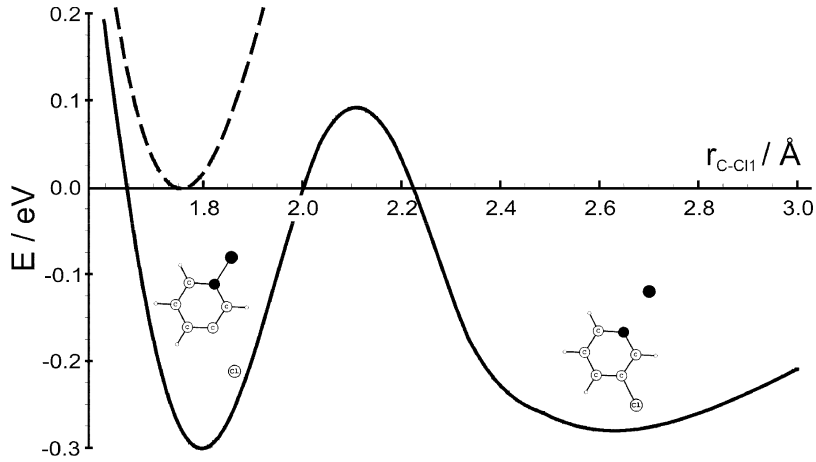

Figure 11. Potential energy as a function of the C1−Cl_1 distance for 1,3-ΦCl_2: neutral molecule (− − −) and anion (—). Geometrical degrees of freedom except the C−Cl_1 distance are relaxed. The molecular geometries corresponding to the minima in the anionic curve are plotted above them. Cl_1 and the connected C atom are shown in black.

example, been done in ref 17 for acetylene with a complex potential or in ref 15 with an additive scheme to approximate the energy.

We calculated the energy along the C−Cl coordinate for the neutral molecule and the anion with the B3LYP density functional and the 6-311++G (d,p) basis set. The C−Cl_1 distance was varied by allowing all other degrees of freedom to relax. The result is shown for the 1,3 isomer in Figure 11. It can be seen that the energy of the anion is lower than the one of the neutral if one of the C−Cl bonds is sufficiently elongated. The two minima in the anionic energy appear when either the C−Cl_1 or the C−Cl_2 distance has a value about 2.6 Å, and they are separated by an unfavorable region with smaller values (2.1 Å) for both of them. The slight difference in the depths of the two minima is an artifact from our point spacing and convergency problems at long C−Cl distances.

The other two isomers give very similar potential energy curves and therefore are not plotted. It is likely that there are no differences of the potential energy curves between the isomers but the different out-of plane vibrational modes that are a consequence of the isomer geometries are responsible for the differences in the reaction rates of the three isomers.

Acknowledgment. This work is supported in part by the FWF (P18804) and by the Austrian Ministry of Science BMWF as part of the Uni-Infrastrukturprogramm of the Forschungsplattform Scientific Computing at LFU Innsbruck. S.D. gratefully acknowledges an APART grant from the Austrian Academy of Sciences.

References and Notes

(1) Christophorou, L. G., Ed.; *Electron-Molecule Interactions and Their Applications*; Academic Press: Orlando, FL, 1984.
(2) Smith, D.; Spanel P. In *Adv. At. Mol. Opt. Phys.*, Academic Press: New York, 1993; Vol. 32.
(3) Larson, R. A.; Weber, E. J. *Reaction Mechanisms in Environmental Organic Chemistry*; CRC Press: Boca Raton, Fl, 1994, p 171.
(4) Massey, H. S. W. *Negative Ions*; Cambridge University Press: Cambridge, 1976.
(5) Illenberger, E.; Momigny, J. *Gaseous Molecular Ions: An Introduction to Elementary Processes Induced by Ionization*; Steinkopff/Springer: Darmstadt/New York, 1992.

(6) Grill, V.; Drexel, H.; Sailer, W.; Lezius, M.; Märk, T. D. *Int. J. Mass Spectrom.* **2001**, *205*, 209–226.
(7) Stamatovic, A.; Schulz, G. *Rev. Sci. Instrum.* **1968**, *39*, 1752.
(8) Kopyra, J.; Szamrej, I.; Graupner, K.; Graham, L. M.; Field, T. A.; Sulzer, P.; Denifl, S.; Märk, T. D.; Scheier, P.; Fabrikant, I. I.; Braun, M.; Ruf, M.-W.; Hotop, H. *Int. J. Mass Spectrom.* **2008**, *277*, 130–141.
(9) Curtiss, L. A.; Redfern, P. C.; Raghavachari, K.; Rassolov, V.; Pople, J. A. *J. Chem. Phys.* **1999**, *110*, 4703.
(10) Fabrikant, I. I.; Hotop, H. *J. Chem. Phys.* **2008**, *128*, 124308.
(11) Burrow, P. D.; Modelli, A.; Jordan, K. *Chem.Phys.Lett.* **1986**, *132*, 441.
(12) Miller, T. M.; Viggiano, A. A.; Friedman, J. F. *J. Chem. Phys.* **2004**, *121*, 9993–9998.
(13) Clarce, D. D.; Coulson, C. A. *J. Chem. Soc. A* **1969**, 169.
(14) Modelli, A.; Venuti, M. *J. Phys. Chem. A* **2001**, *105*, 5836.
(15) Skalicky, T.; Chollet, C.; Pasquier, N.; Allan, M. *Phys. Chem. Chem. Phys.* **2002**, *4*, 3583.
(16) Laage, D.; Burghardt, I.; Sommerfeld, T.; Hynes, J. T. *ChemPhysChem* **2003**, *4*, 61.
(17) Chourou, S. T.; Orel, A. E. *Phys. Rev. A* **2008**, *77*, 042709.

JP9050726